Half-Sandwich Structure of Cyclopentadienyl Dialuminum [$Al_2(\eta^5\text{-}C_5H_5)$] from Pulsed-Field Ionization Electron Spectroscopy and ab Initio Calculations

Yuxiu Lei and Dong-Sheng Yang*

Department of Chemistry, University of Kentucky, Lexington, Kentucky 40506-0055

Received: August 13, 2007; In Final Form: November 28, 2007

Cyclopentadienyl dialuminum [Al_2Cp, $Cp = C_5H_5$] was prepared in a pulsed laser ablation cluster beam source and identified with a time-of-flight photoionization mass spectrometer. The high-resolution electron spectrum of this complex was obtained using pulsed-field ionization zero electron kinetic energy (ZEKE) photoelectron spectroscopy. Three isomeric structures with two Al atoms residing on the same or opposite sites of the Cp plane were predicted by second-order Møller−Plesset perturbation theory. A half-sandwich structure with an aluminum dimer perpendicular to the Cp plane was identified by the experiment. The ground electronic states of the neutral and ionized species are $^2A''$ in C_s symmetry and $^1A_1$ in C_{5v} symmetry, respectively. In both the neutral and ionic states, one of the Al_2 atoms binds with five carbons, and the metal−ligand bonding consists of orbital and electrostatic contributions. Ionization of the $^2A''$ neutral state enhances the metal−ligand bonding but weakens the metal−metal interaction.

1. Introduction

Metallocenes play a central role in organic and organometallic synthesis[1] and chemical catalysis.[2] Compared to transition metal cyclopentadienyl (Cp) complexes where metal (M) atoms are strongly bound in a fivefold η^5 mode, the binding between main group elements and Cp is generally weaker and more diverse. It ranges from η^1 to η^5 and from highly ionic to largely covalent character across the periodic table.[3−6] The π-complexes of the main group elements have been known to include discrete [MCp_n]($n = 1-3$) molecules, polymeric structures with [...M−Cp−M...] backbone strands, and [$MCp]_n$ ($n = 4-6$) clusters.[3−7]

In 1991, Schnöckel and co-workers reported the synthesis and structure of the first (pentamethylcyclopentadienyl)aluminum(I) compound, [$(AlCp^*)_4$, $Cp^* =$ pentamethylcyclopentadienyl].[8] In the solid state, room-temperature X-ray crystallography showed that the tetrameric compound consisted of a tetrahedral Al_4 core. Each Al atom in this tetrahedron was η^5 bonded to a terminal Cp* ring, and each Cp* ring plane was parallel to an opposite Al_3 face.[8] In the toluene solution, ^{27}Al NMR spectra recorded in the temperature range −80 to +25 °C indicated the complex to be a tetramer. Above 30 °C, the ^{27}Al NMR spectroscopy showed the existence of both the tetramer and monomer, and the concentration of the monomer increased with increasing temperatures. Analysis of the temperature dependence of the ^{27}Al NMR spectra yielded the dissociation energy of 150(20) kJ mol^{-1} for the process $[AlCp^*]_4 \rightarrow 4AlCp^*$.[9] In the gas phase, an electron diffraction study at 139(4) °C showed that the tetramer was decomposed into monomeric units, consistent with the observation of solution NMR spectroscopy.[10] A more recent mass spectrometric study, however, yielded different observations from those of the NMR and electron diffraction studies.[11] In that mass spectrometric study, the $[AlCp^*]_4$ compound was laser vaporized and ionized, and the resulting ions were determined with Fourier transform ion cyclotron resonance mass spectrometry. These ion signals corresponded to $[Al_xCp_y^*]^+$ ($x \geq y$), with the strongest signal belonging to $[Al_2Cp^*]^+$. The monomeric $[AlCp^*]^+$ signal was only about 8% of $[Al_2Cp^*]^+$. Encouraged by the success with the (pentamethylcyclopentadienyl)aluminum(I) compound, Schnöckel and co-workers have also attempted to isolate the parent cyclopentadienylaluminum(I) compound, but such experiments were not successful due to its low thermal stability.[10]

In this paper, we report pulsed-field ionization-zero electron kinetic energy (ZEKE) photoelectron spectroscopy of cyclopentadienyl dialuminum [Al_2Cp, Cp = cyclopentadienyl]. The ZEKE spectroscopy, combined with second-order Møller−Plesset (MP2) calculations, shows that the Al_2Cp complex is in a mixed-valent half-sandwich structure. In this structure, an Al atom is directly bound to the Cp ligand in a η^5 fashion, whereas the other Al atom acts like a spectator. To our knowledge, this is the first gaseous mixed-valent cyclopentadienyl metal complex characterized spectroscopically, and it represents an interesting binding configuration.

2. Experimental and Computational Methods

Our metal cluster beam ZEKE spectrometer was described in a previous publication.[12] The Al_2Cp complex was formed in a pulsed supersonic molecular beam. The aluminum was introduced into the gas phase by pulsed laser ablation of an Al rod (99.9%, Alfa Aesar). Reaction with gaseous cyclopentadiene, produced by distillation of dicyclopentadiene (Aldrich) at 210−220 °C, in this high-energy environment led to production of the Al_2Cp complex. The mechanism leading to formation of this complex is unknown at the present time, but it likely involves the reaction of an Al dimer with a Cp radical. Laser ablation was carried out with the second harmonic output of a Nd:YAG laser (Lumonics YM-800, 532 nm, 0.5 mJ). During the experiment, the Al rod was continuously translated and rotated by a motor-driven device to ensure each laser pulse ablated a fresh metal surface; cyclopentadiene liquid was kept at about 0 °C to minimize dimerization and stabilize the vapor pressure of the ligand. The Al_2Cp complex and other species formed in the molecular beam were seeded in a He/Ar carrier gas mixture and expanded to the vacuum chamber. The gas

* Corresponding author. E-mail: dyang0@uky.edu.

10.1021/jp076507e CCC: $40.75
Published on Web 01/26/2008

mixture had a reservoir pressure of ~60 psi and was delivered by a piezoelectric pulsed value.[13] The gas pulses were synchronized with the laser pulses to optimize the production of the Al_2Cp complex.

Charged species in the molecular beam were removed by a dc electric field before they entered into the spectroscopy chamber, neutral products were identified with photoionization time-of-flight mass spectrometry, and the ionization threshold of Al_2Cp was located by photoionization efficiency (PIE) spectroscopy. Prior to ZEKE experiments, the production of $[Al_2Cp]^+$ was maximized by adjusting the timing and power of the vaporization and ionization lasers and backing pressure of the carrier gas. ZEKE electrons were generated by photoexcitation of neutral molecules to high-lying Rydberg states, followed by delayed pulsed electric field (4 μs delay, 1.2 V/cm strength, and 100 ns width) ionization of these Rydberg states. A small dc field (~0.08 V/cm) was applied to help discriminate ZEKE electrons from kinetic electrons produced by photoionization. The photoionization and photoexcitation laser was the doubled-frequency output of a dye laser (Lumonics HD-500) pumped by the third harmonic of a Nd:YAG laser (Continuum Surelite-II, 355 nm). A delay generator (Stanford Research Systems DG535) provided the pulsed electric field for ionization. The ion and electron signals were detected by a dual microchannel plate detector (Burle), amplified by a preamplifier (Stanford Research Systems SR445), averaged by a gated integrator (Stanford Research Systems SR250), and stored in a laboratory computer. Laser wavelengths were calibrated against titanium atomic transitions in the frequency range of the ZEKE spectrum.[14] The field dependence of ZEKE peak positions could not be measured for this complex due to the limited size of the ZEKE signal. However, the field-induced energy shift for this complex is likely smaller than the spectral line width, as shown by previous ZEKE measurements of $Cr(C_6H_6)_2$.[15]

Geometries and vibrational frequencies of Al_2Cp and $[Al_2Cp]^+$ were calculated with the MP2 method and 6-311+G(d,p) basis set, implemented in the GAUSSIAN03 program.[16] Multidimensional Franck-Condon (FC) factors of vibrational transitions from Al_2Cp to $[Al_2Cp]^+$ electronic states were computed using the theoretical equilibrium geometries, harmonic vibrational frequencies, and normal mode coordinates of the neutral and ionic complexes.[17,18] The Duschinsky effect was considered to account for normal mode differences between the neutral and ionic states in the FC calculations.[19] Spectral broadening was simulated by giving each line a Lorentzian line shape with the experimental spectral line width. Transitions from excited vibrational levels of the neutral complex were simulated by assuming thermal excitations at specific temperatures.

3. Results and Discussion

A. Photoionization Efficiency and ZEKE Spectra. Figure 1 presents the photoionization efficiency (PIE) spectrum of Al_2Cp seeded in a He/Ar (1:1) mixture. The ionization threshold determined from the sharp onset of the ion signal is 40 700(50) cm^{-1}. This value was corrected by +110 cm^{-1}, the energy shift induced by a dc extraction field of 320 V cm^{-1}. The ionization threshold from the PIE measurement was used to simplify the ZEKE experiment and correlate with ZEKE signals.

Figure 2a shows the ZEKE spectrum of Al_2Cp also seeded in a He/Ar (1:1) mixture. Peaks from single vibrational-mode excitations are labeled in the figure, and others are easily assigned to transitions involving two or more vibrational modes. The first strong peak appears at 40 690(5) cm^{-1} [5.0449(6) eV] and is the origin (0−0) of the electronic transition between the ground vibrational levels of the neutral and ionized complexes. Above the origin of the electronic transition, the spectrum exhibits 1082 and 851 cm^{-1} intervals and a main vibrational progression of 482 cm^{-1} separations. Nested inside the 482 cm^{-1} progression are 175 and 50 cm^{-1} intervals, respectively. All these transitions correspond to vibrational excitations in the ionized complex. In addition, another 50 cm^{-1} vibrational progression begins from a small peak at 24 cm^{-1} below the 0−0 transition. The intensities of these peaks depended on the condition of the molecular beam, and they are attributed to transitions from excited vibrational levels of the neutral complex to various vibrational levels of the 50 cm^{-1} mode in the ion. By comparison to the vibrational frequencies of gaseous Cp[20,21] ligand and MCp (M = Mg, Ca, Sr, Zn, and Cd) complexes[22−26]

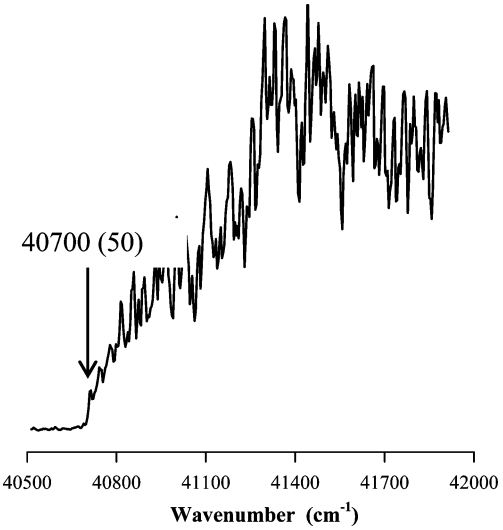

Figure 1. Photoionization efficiency curve of Al_2Cp seeded in a He/Ar (1:1) mixture.

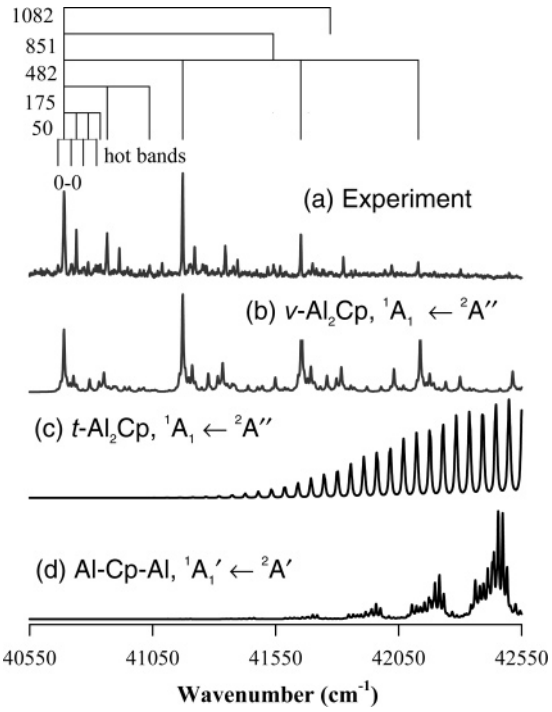

Figure 2. ZEKE spectrum of Al_2Cp seeded in a He/Ar (1:1) mixture (a) and simulations of singlet ← doublet transitions of the v-Al_2Cp (b), t-Al_2Cp (c), and Al−Cp−Al (d) isomers at 50 K. The transition in (c) represents ionization of the $^2A''$ state of t-Al_2Cp leading to the $^1A_1$ state of [v-Al_2Cp]$^+$.

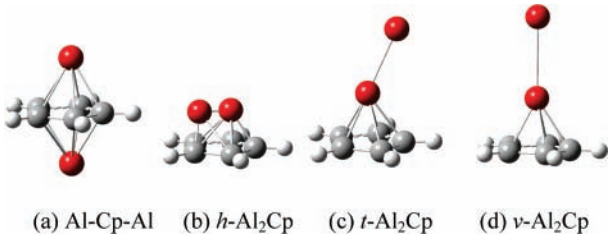

Figure 3. Structural isomers of Al_2Cp.

TABLE 1: Electronic States and Relative Energies (E_e) of Various Isomers of Cyclopentadienyl Dialuminum from MP2/6-311+G(d,p) Calculations

isomers	states	E_e (eV)
v-Al_2Cp		
C_s	$^2A''$	0.01
C_{5v}	$^4A_1$	1.00
[v-Al_2Cp]$^+$		
C_{5v}	$^1A_1$	4.71
C_s	$^3A''$	6.41
t-Al_2Cp[a]		
C_s	$^2A''$	0
Al−Cp−Al		
C_s	$^2A'$	0.09
C_s	$^4A''$	2.43
[Al−Cp−Al]$^+$		
D_{5h}	$^1A_1'$	4.13
C_1	^3A	7.27

[a] The singlet, triplet, and quartet states of t-Al_2Cp were converged to the corresponding states of v-Al_2Cp. The t-Al_2Cp doublet state has the Al−Al bond tilt about 60° against Cp plane.

and solid compounds of CpBeCl,[27] InCp,[28] KCp,[29] $FeCp_2$,[30] and $ZnCp_2$,[31] the observed 1082 and 851 cm^{-1} intervals may be assigned to ligand-based vibrations, whereas the 482, 175, and 50 cm^{-1} intervals may be attributed to metal−ligand and metal−metal vibrations. The 175 cm^{-1} spacing is close to the predicted Al−Al stretch frequency (169 cm^{-1}) of the Al_2 $^2\Sigma_g^+$ ground state[32,33] and may thus be assigned to the excitation of the Al−Al stretching mode of the [Al_2Cp]$^+$ ion. The observation of the Al−Al stretch indicates that the Cp radical binds with an Al_2 dimer, rather than two separate Al atoms. In the following sections, we will discuss detailed spectral analysis and structures of the Al_2Cp complex.

B. Structural Isomers. Figure 3 presents four possible structural isomers of Al_2Cp with Al atoms residing on the same or opposite sides of the Cp ring. Al−Cp−Al (Figure 3a) is an inverse sandwich structure with Al atoms on opposite sides of the Cp ring. This type of structure is the building block of common polymeric [MCp]$_x$ compounds in the solid state.[6] Three other isomers (Figure 3b−d) contain Al atoms residing on the same side of the Cp ring, with Al_2 being horizontal (h-Al_2Cp), tilted (t-Al_2Cp), or vertical (v-Al_2Cp) to the Cp plane, respectively.

The inverse sandwich structure is formed by the Cp ring binding to two isolated Al atoms, and the other structures are formed by Cp binding to Al_2. The ground electronic state of Cp is known as $^2E_1''$ (D_{5h}) with an electron configuration of $(a_2'')^2(e_1'')^3$ and is subjected to a Jahn−Teller distortion.[20,21] Each Al atom has a $3p^1$ electron in its ground electron configuration, and the ground electronic state of Al_2 is $^3\Pi_u$ with a $\sigma^1\pi^1$ configuration.[32−36] The interaction of two Al atoms or an Al_2 dimer with a Cp radical is thus expected to form Al_2Cp in doublet/quartet neutral states and singlet/triplet ionic states. Table 1 lists the relative energies of these spin states for the Al−Cp−Al, t-Al_2Cp, and v-Al_2Cp isomers predicted by the MP2/6-311+G(d, p) calculations. The h-Al_2Cp initial structure did not survive from the geometry optimization and was converged to t-Al_2Cp. For the t-Al_2Cp isomer, the MP2 calculations located only a doublet state, and other spin states were converged to the corresponding spin states of v-Al_2Cp. For v-Al_2Cp and Al−Cp−Al, the theory found the doublet and quartet states for the neutral complex and the singlet and triplet states for the ion. The doublet state of the neutral complex is more stable than the quartet state, whereas the singlet ion is more stable than the triplet ion. The lower energy of the doublet state may be understood by considering frontier orbital interactions between the Al atoms (or Al_2 dimer) and Cp radical. For example, if an Al $3p^1$ electron fills in the highest occupied molecular orbital (HOMO) [$(e_1'')^3$] of the Cp radical, and the other Al $3p^1$ electron remains to be metal-based, the resulting complex should be in a doublet spin state. On the other hand, if both the Al and Cp ground electron configurations remain unchanged upon metal−ligand coordination, the complex should be in a quartet spin state. Because the Al $3p^1$ electron [IE(Al) = 5.9858 eV[37]] has higher energy than the e_1'' π electron of the Cp radical [IE(Cp) = 8.4272 eV],[38] the doublet state of Al_2Cp is expected to be more stable than its quartet state. Similar considerations can be used to rationalize the relative stability of the singlet and triplet ions. Among the doublets of the three isomers, their energy differences are predicted to be less than 0.1 eV (Table 1). This is in contrast to pentamethylcyclopentadienyl dialuminum (Al_2Cp^*), where the inverse sandwich isomer with Al on opposite sides of the Cp* plane was calculated to be about 0.3 eV more stable than the half-sandwich isomer with two Al atoms on the same side.[11]

TABLE 2: Adiabatic Ionization Energies (IE), Including Vibrational Zero-Point Energy Corrections, of Various Isomers of Cyclopentadienyl Dialuminum from MP2/6-311+G(d,p) Calculations

electronic transitions	IE (eV)[b]
[v-Al_2Cp]$^+$ ← v-Al_2Cp	
$^1A_1$ (C_{5v}) ← $^2A''$ (C_s)	5.11
$^3A''$ (C_s) ← $^2A''$ (C_s)	6.77
$^3A''$ (C_s) ← $^4A_1$ (C_{5v})	5.73
[v-Al_2Cp]$^+$ ← t−Al_2Cp[a]	
$^1A_1$ (C_{5v}) ← $^2A''$ (C_s)	5.09
$^3A''$ (C_s) ← $^2A''$ (C_s)	6.75
[Al−Cp−Al]$^+$ ← [Al−Cp−Al]	
$^1A_1'$ (D_{5h}) ← $^2A'$ (C_s)	4.42
^3A (C_1) ← $^2A'$ (C_s)	7.53
^3A (C_1) ← $^4A''$ (C_s)	5.19

[a] The neutral t-Al_2Cp isomer is converted to the ionic v-Al_2Cp upon ionization. [b] The calculated IE values were corrected by +0.36 eV, the averaged MP2 computational error for the IEs of metal association complexes.[39−43]

C. Observed Structural Isomer and Electronic Transition. From the MP2 calculations, the ground state of the Al_2Cp complex appears to be a doublet spin state. However, because the energy differences among the doublets of the three isomers are so small (Table 1), the theory is unable to establish the preferred structure. To determine the structure of this complex, we shall compare theoretical and experimental IEs, vibrational frequencies, and spectral intensities. Table 2 lists the theoretical IEs of v-Al_2Cp, t-Al_2Cp, and Al−Cp−Al. These IE values were corrected by +0.36 eV, the averaged error of MP2/6-311+G-(d,p) calculations on the IEs of other metal−ligand association complexes.[39−43] The calculated IE values of the $^1A_1$ ← $^2A''$ transitions of v-Al_2Cp and t-Al_2Cp and the ^3A ← $^4A''$ transition of Al−Cp−Al are close to the experimental value of 5.0449 (6) eV, whereas the calculated IE values of all other transitions are either too high or too low. Moreover, the quartet states of both v-Al_2Cp and Al−Cp−Al are predicted to be at least 1.0

TABLE 3: Peak Positions (cm^{-1}) and Assignment of the $Al_2CpZEKE$ Spectrum

position	assignment	rel position[a]	position	assignment	rel xposition[a]
40666	17_1^0	−24	41295	$17_2^0 4_0^1 5_0^1$	605
40690	0−0	0	41316	$4_0^1 17_0^3$	626
40721	$30_1^0 17_0^1$	31	41345	$4_0^1 5_0^1$	655
40740	17_0^1	50	41378	$30_1^0 4_0^1 5_0^1 17_0^1$	688
40770	$30_1^0 17_0^2$	80	41395	$4_0^1 5_0^1 17_0^1$	705
40787	17_0^2	97	41473	$17_2^0 4_0^1 5_0^2$	783
40811	17_1^3	121	41518	$4_0^1 5_0^2$	828
40822	$30_1^0 17_0^3$	132	41541	3_0^1	851
40829	$30_2^0 5_0^1$	139	41569	$4_0^1 5_0^2 17_0^1$	879
40837	17_0^3	147	41593	$3_0^1 17_0^1$	903
40865	5_0^1	175	41652	4_0^2	962
40915	$5_0^1 17_0^1$	225	41684	$30_1^0 4_0^2 17_0^1$	994
40949	$30_1^0 5_0^1 17_0^2$	259	41700	$4_0^2 17_0^1$	1010
40965	$5_0^1 17_0^2$	275	41716	$3_0^1 5_0^1$	1026
40998	$30_1^0 5_0^1 17_0^3$	308	41740	$4_0^2 17_1^2$	1050
41014	$5_0^1 17_0^3$	324	41747	$4_0^2 17_0^2$	1057
41037	5_0^2	347	41772	2_0^1	1082
41070	$30_1^0 5_0^2 17_0^1$	380	41825	$4_0^2 5_0^1$	1135
41089	$5_0^2 17_0^1$	399	41857	$30_1^0 4_0^2 5_0^1 17_0^1$	1167
41116	$30_2^0 17_1^0 4_0^1$	426	41874	$4_0^2 5_0^1 17_0^1$	1184
41172	4_0^1	482	41994	$4_0^2 5_0^2$	1304
41202	$30_1^0 4_0^1 17_0^1$	512	42022	$3_0^1 4_0^1$	1332
41221	$4_0^1 17_0^1$	531	42130	4_0^3	1440
41253	$30_1^0 4_0^1 17_0^2$	563	42194	$3_0^1 4_0^1 5_0^1$	1504
41259	$30_2^0 17_2^0 4_0^1 5_0^1$	569	42301	$4_0^3 5_0^1$	1611
41270	$4_0^1 17_0^2$	580	42499	$3_0^1 4_0^2$	1809

[a] Relative positions are referenced to the position of the 0−0 transition at 40 690 cm^{-1}.

TABLE 4: Measured and Calculated Adiabatic Ionization Energies (IE, eV) and Vibrational Frequencies (cm^{-1}) of the Half-Sandwich Structure of Cyclopentadienyl Dialuminum[a]

	ZEKE	MP2
IE [$^1A_1$ (C_{5v}) ← $^2A''$ (C_s)]	5.0449 (6)	5.11[b]
C−C stretch (a_1, ν_2^+)	1082	1136
CH wag (a_1, ν_3^+)	851	859
Al−Cp stretch (a_1, ν_4^+)	482	483
Al−Al stretch (a_1, ν_5^+)	175	162
Al−Cp bend (e_1, $\nu_{17,18}^+$)	50	52
Al−Cp bend (a'/a'', ν_{17}/ν_{30})	24/19	13/41

[a] ν^+ and ν represent the vibrational modes in the ionic $^1A_1$ and neutral $^2A''$ states, respectively. [b] The calculated IE values were corrected by +0.36 eV, the averaged MP2 computational error for the IEs of metal association complexes.[39−43]

eV higher in energy than their doublet states (Table 1). Therefore, these quartet states should not be populated under supersonic expansion conditions, and the $^3A'' \leftarrow {}^4A_1$ transition of v-Al_2Cp and the $^3A \leftarrow {}^4A''$ transition of Al−Cp−Al can thus be excluded from the observed spectrum. Because their IE values are predicted to be too high, the triplet ← doublet transitions of all three isomers can be excluded from the experimental spectrum as well. Therefore, only the singlet ← doublet transitions are possible.

Parts b−d of Figure 2 show the spectral simulations of singlet ← doublet transitions in comparison with the experimental spectrum. In these simulations, vibrational frequencies were not scaled, but the ionization energy was shifted to the experimental value for easier comparison of the measured and calculated vibrational frequencies and spectral profiles. The simulation from the v-Al_2Cp structure (Figure 2b) matches the experimental spectrum reasonably well, and those from t-Al_2Cp (Figure 2c) and Al−Cp−Al (Figure 2d) exhibit too long FC profiles due

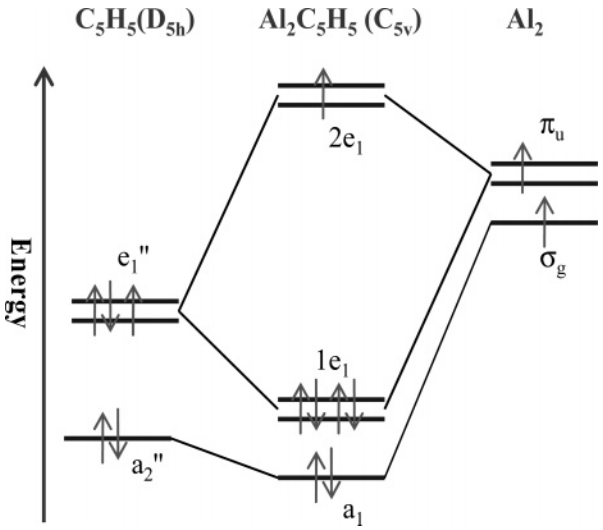

Figure 4. Qualitative molecular orbital diagram of v-Al_2Cp constructed from the outer valence orbitals of Cp and Al_2.

to large differences between the neutral and ionic geometries. Simulations (not shown) of the triplet ← doublet and triplet ← quartet transitions of the three isomers display no similarity to the measured spectrum either. Thus, these comparisons clearly show that observed spectrum originates from the $^1A_1 \leftarrow {}^2A''$ transition of the half-sandwich v-Al_2Cp complex. With the good agreement between the simulation and the experimental spectrum, we can now make a detailed spectral assignment. The 1082 and 851 cm^{-1} intervals are assigned to vibrations of the C−C stretch (or ring breathing mode) (ν_2^+, a_1) and CH wag (ν_3^+, a_1) of the Cp ring, and the 482, 175, and 50 cm^{-1} progressions above the 0−0 transition are attributed to excitations of the Al-Cp stretch (ν_4^+, a_1), Al−Al stretch (ν_5^+, a_1), and Al-Cp bend (ν_{12}, e_1) in the ionic $^1A_1$ state, respectively. In addition, the second 50 cm^{-1} progression beginning from the 24 cm^{-1} peak below the 0−0 transition is assigned to the transitions from the excited vibrational levels of the $^2A''$ state. By combing the two 50 cm^{-1} progressions, we obtain the vibrational frequencies of 24 and 19 cm^{-1} for the two Al-Cp bending motions (ν_{17}/ν_{30}, a'/a'') in the $^2A''$ state. It is noted that the Al-Cp bend is doubly degenerate (e_1) in the $^1A_1$ (C_{5v}) ion state and splits into two nondegenerate modes (a' and a'') in the $^2A''$ (C_s) neutral state. In the zeroth-order approximation based on the harmonic oscillator and one-to-one correspondence of normal mode coordinates, one would expect little intensity of the doubly degenerate e_1 ion mode transitions that involve an odd quantum number [i.e., $\Delta(\nu^+ - \nu) = \pm 1, \pm 3, \pm 5$]. However, our calculations indicate a rotation of the normal coordinates of the e_1 ion mode with respect to the corresponding a' and a'' neutral modes. This rotation leads to the e_1 ion mode being a mixture of the a' and a'' neutral modes (Duschinsky effect). Because of this mode mixing, transitions involving an arbitrary number of quanta of either components of the e_1 ion mode are possible, as confirmed by the FC factor calculations. Table 3 lists the complete assignment for each observed ZEKE transition. Compared to the free Cp radical ($\nu_{C-C\ stretch} = 1081$ cm^{-1} and $\nu_{CHwag} = 681$ cm^{-1}),[20,21] the C−C stretch frequency (1082 cm^{-1}) is comparable but the CH wag frequency (852 cm^{-1}) is much higher in this complex, as observed for other cyclopentadienyl metal complexes.[23,27−31] Compared to the free Al_2, the Al−Al stretch frequency (175 cm^{-1}) in this complex is close to that of the ionic $Al_2^+ {}^2\Sigma_g^+$ ground state (169 cm^{-1})[33] but is much lower than that of the neutral $Al_2 {}^3\Pi_u$ ground state (286 cm^{-1}).[34−36]

TABLE 5: Bond Distances (Å) of v-Al_2Cp, Al_2, and Cp from MP2/6-311+G(d,p) Calculations

molecules	states	Al−Al	Al−C_1	Al−C_2	Al−C_3	Al−C_4	Al−C_5	C_1−C_2	C_2−C_3	C_3−C_4	C_4−C_5	C_5−C_1
v-Al_2Cp	$^2A''$	2.814	2.306	2.313	2.308	2.308	2.313	1.426	1.422	1.428	1.422	1.426
$[v\text{-}Al_2Cp]^+$	$^1A_1$	2.984	2.220	2.220	2.220	2.220	2.220	1.429	1.429	1.429	1.429	1.429
Al_2[a]	$^3\Pi_u$	2.704										
Al_2^+	$^2\Sigma_g^+$	3.213										
Cp[b]	$^2B_1$							1.442	1.355	1.452	1.355	1.442

[a] The Al−Al bond length of the Al_2 ($^3\Pi_u$) from a rotational analysis is 2.701 ± 0.002 Å.[34] [b] The C−C bond length of Cp ($^2E_1''$) from a rotational analysis is 1.421 ± 0.001 Å;[47] the C−C bond lengths of Jahn−Teller distorted Cp ($^2B_1$) from a vibronic analysis are 1.416, 1.404, and 1.435 Å.[21] The C−C bond length in the Cp^- anion ($^1A_1'$) is predicted to be 1.419 Å by our MP2/6-311+G(d,p) calculations.

Table 4 summarizes the measured and calculated IEs and vibrational frequencies. The MP2 calculations underestimate the IE value by 0.29 eV, which is slightly smaller than the averaged MP2 computational errors (0.36 ± 0.05 eV) for the IEs of other metal association complexes.[39−43] The calculated frequencies are generally in excellent agreement with the measured values, expect for the very soft metal−ligand bending modes (ν_{17} and ν_{30}) in the $^2A''$ state.

D. Bonding of the Half-Sandwich v-Al_2Cp Complex. Previous studies have shown that bonding interactions between Cp and main group elements are highly ionic for group 1 elements and largely covalent for groups 14 and 15 elements, with complexes of other main group elements exhibiting various degrees of ionic and covalent character.[6]

In Figure 4, we show a qualitative molecular orbital diagram of v-Al_2Cp constructed from the valence orbitals of Cp and Al_2 ground states and by assuming the geometry of the complex to be in the C_{5v} point group. The Cp e_1'' orbital is placed in lower energy than the Al_2 π_u orbital because the first ionization energy of the organic moiety (8.4272 eV)[38] is higher than that of the metal dimer (5.6, 5.8, or 6.0−6.4 eV).[44−46] The energy separation between the e_1'' and a_2'' orbitals of Cp is assumed to be larger than that between the π_u and σ_g orbitals of Al_2. This is because the bonding features of the Cp e_1'' (partially antibonding among C 2pπ orbitals) and a_2'' orbitals (bonding among all C 2pπ orbitals) are rather different, whereas the Al_2 π_u and σ_g orbitals are quite similar (both with an Al 2p electron). The π_u orbital of the Al_2 dimer is of e_1 representation when labeled in C_{5v} and interacts with the e_1'' orbital of the Cp moiety. Similarly, the σ_g orbital of Al_2 is of a_1 symmetry in C_{5v} and can interact with the a_2'' orbital of Cp. Because the Al_2 π_u and σ_g orbitals have higher energies than the Cp e_1'' and a_2'' orbitals, these interactions stabilize the ligand orbitals and destabilize the metal orbitals. The highest occupied molecular orbital ($2e_1$) of v-Al_2Cp remains a largely Al_2 pπ character but has higher energy than the π_u orbital of Al_2. This explains why the IE of the v-Al_2Cp [5.0449(6) eV] is lower than that of the Al_2 dimer (5.6, 5.8, or 6.0−6.4 eV).[44−46] Energies of the $1e_1$ and a_1 orbitals of the complex depend on the strength of relevant orbital interactions, and their energy order may be different from what is shown in Figure 4. On the basis of the qualitative orbital analysis, the complex would have a $^2E_1$ ground state in C_{5v}, but the orbital degeneracy is lifted by the Jahn−Teller effect, resulting in a $^2A''$ ground state. Presumably, a second Jahn−Teller component should be in a $^2A'$ state and lie close to the $^2A''$ component, but it was not located by our calculations. In the $^2A''$ ground state, the Al−C distances are predicted to be 2.306 − 2.313 Å, and the C−C distances are 1.422 − 1.428 Å (Table 5). Although the predict Al−C (and C−C) bond distances differ slightly, these differences are significant as our calculations with C_{5v} restriction failed to converge.

Along with these orbital interactions, electrostatic interactions play a large role as well. Table 6 presents the natural charges and electron configurations of v-Al_2Cp, Al_2, and Cp from the natural population analysis. This analysis shows a significant charge transfer from the Al_a atom that binds directly with the Cp radical. As a result, the Al_a atom bears a positive charge (0.59), and the Cp ligand has a negative charge (−0.54). However, the Al_b atom that is not directly bound to Cp remains essentially a zero-charge. The natural electron configurations are predicted to be $3s^{1.52}3p^{0.86}$ for Al_a and $3s^{1.91}3p^{1.13}$ for Al_b in v-Al_2Cp ($^2A''$). The later is almost identical to the Al electron configuration $3s^{1.88}3p^{1.10}$ in the ground state of Al_2 ($^3\Pi_u$). Due to the depletion of the electron density on one of the Al atoms (and thus between the Al atoms), the Al−Al bond is weakened, and its bond length is increased from 2.704 to 2.814 Å upon Cp coordination. Because the two Al atoms in the complex carry rather different electric charges, the half-sandwich v-Al_2Cp may be considered as a mixed-valent complex, as it is expected by considering their formal oxidation states.

TABLE 6: Natural Charges and Electron Configurations in v-Al_2Cp, Al_2, and Cp from the Natural Population Analysis of MP2/6-311+G(d,p)[a]

molecules	charges	electron configurations
v-Al_2Cp ($^2A''$, C_s)		
Al_a	0.59	$3s^{1.52}3p^{0.86}$
Al_b	−0.05	$3s^{1.91}3p^{1.13}$
Cp	−0.54	$2s^{0.96}2p^{3.34}$
ν−$[Al_2Cp]^+$ ($^1A_1$, C_{5v})		
Al_a	0.54	$3s^{1.37}3p^{1.07}$
Al_b	0.79	$3s^{1.97}3p^{0.24}$
Cp	−0.33	$2s^{0.97}2p^{3.31}$
Al_2 ($^3\Pi_u$, $D_{\infty h}$)	0.00	$3s^{1.88}3p^{1.10}$
Al_2^+ ($^2\Sigma_g^+$, $D_{\infty h}$)	1.00	$3s^{1.95}3p^{0.55}$
Cp ($^2B_1$, C_{2v})	0.0	$2s^{0.97}2p^{3.20}$

[a] The electron configurations of the Cp radical are represented by those of the C atoms. Al_a is referred to the Al atom that binds directly to Cp, whereas Al_b has no direct binding with the ligand.

The ground state of the v-$[Al_2Cp]^+$ ion is $^1A_1$ in C_{5v} symmetry and is formed by removal of the Al_2-based pπ electron of the $^2A''$ state. In this singlet ion state, the electron configurations or electric charges of the carbon and Al_a atoms are rather similar to those of the doublet neutral state. On the other hand, the electron configuration of Al_b experiences a dramatic change from $3s^{1.91}3p^{1.13}$ in the $^2A''$ state to $3s^{1.97}3p^{0.24}$ in the $^1A_1$ state, and the electric charge of Al_b is increased from −0.05 in the $^2A''$ state to 0.79 in the $^1A_1$ state. These changes in the electron configuration and electric charge suggest that ionization removes an electron largely from the Al_b 3p orbital (mixed with the Cp e'' character in an antibonding fashion). As the electron density decreases, the Al−Al bonding becomes weaker in the ion. This bond weakening is evident from the increase of the Al−Al distance from 2.814 to 2.984 Å upon ionization.

4. Conclusions

We have reported the first joint ZEKE spectroscopic and MP2 computational study of cyclopentadienyl dialuminum. ZEKE

spectroscopy measures the adiabatic IEs and several vibrational frequencies, and MP2 calculations predict a number of low-energy isomers. By comparing the experimental measurements and theoretical calculations, we have determined a half-sandwich structure for the complex. In this structure, the Al_2 dimer is perpendicular to the Cp plane and one of the Al_2 atoms binds with the Cp radical in a η^5 mode. The ground state of the neutral complex is $^2A''$ in C_s symmetry. The metal−ligand bonding in the $^2A''$ state has both orbital and electrostatic contributions. Ionization of the $^2A''$ state removes an electron of the largely Al_2 pπ mixed with Cp π in an antibonding manner and yields a $^1A_1$ state in C_{5v} symmetry. In this singlet state, the metal−ligand bonding becomes stronger due to the removal of the antibonding electron, whereas the metal−metal bonding becomes weaker due to the depletion of the electron density between the two Al atoms.

Acknowledgment. We gratefully acknowledge support from the Experimental Physical Chemistry Program of the National Science Foundation. We also thank partial support from the donors of the Petroleum Research Fund of the American Chemical Society and the Kentucky Science and Engineering Foundation. We thank Jack Selegue for providing us with the dicyclopentadiene distillation setup and for fruitful discussion.

References and Notes

(1) Togni, A., Haltermann, R. L., Eds. *Metallocenes*; Wiley: New York, 1998.

(2) Cornils, B., Herrmann, W. A., Eds. *Homogeneous Catalysis with Organometallic Compounds*; VCH: Weihneim, 1996; Vols. 1 and 2.

(3) Budzelaar, P. H. M.; Engelberts, J. J.; van Lenthe, J. H. *Organometallics* **2003**, *22*, 1562.

(4) Rayon, V. M.; Frenking, G. *Chem. Eur. J* **2002**, *8*, 4693.

(5) Shapiro, P. J. *Coord. Chem. Rev.* **1999**, *189*, 17.

(6) Jutzi, P.; Burford, N. *Chem. Rev.* **1999**, *99*, 969.

(7) Beswick, M. A.; Palmer, J. S.; Wright, D. S. *Chem. Soc. Rev.* **1998**, *27*, 225.

(8) Dohmeier, C.; Robl, C.; Tacke, M.; Schnockel, H. *Angew. Chem., Int. Ed. Engl.* **1991**, *30*, 564.

(9) Gauss, J.; Schneider, U.; Ahlrichs, R.; Dohmeier, C.; Schnoeckel, H. *J. Am. Chem. Soc.* **1993**, *115*, 2402.

(10) Haaland, A.; Martinsen, K.-G.; Shlykov, S. A.; Volden, H. V.; Dohmeier, C.; Schnockel, H. *Organometallics* **1995**, *14*, 3116.

(11) Koch, K.; Burgert, R.; Stosser, G.; Schnockel, H. *Eur. J. Mass Spetrom.* **2005**, *11*, 469.

(12) Sohnlein, B. R.; Li, S.; Fuller, J. F.; Yang, D.-S. *J. Chem. Phys.* **2005**, *123*, 014318.

(13) Proch, D.; Trickl, T. *Rev. Sci. Instrum.* **1989**, *60*, 713.

(14) Moore, C. E. *Atomic Energy Levels*; National Bureau Standards: Washington, DC, 1971.

(15) Sohnlein, B. R.; Yang, D.-S. *J. Chem. Phys.* **2006**, *124*, 134305.

(16) Frisch, M. J.; Trucks, G. W.; Schlegel, H. B.; Scuseria, G. E.; Robb, M. A.; Cheeseman, J. R.; Montgomery, J. A., Jr.; Vreven, T.; Kudin, K. N.; Burant, J. C.; Millam, J. M.; Iyengar, S. S.; Tomasi, J.; Barone, V.; Mennucci, B.; Cossi, M.; Scalmani, G.; Rega, N.; Petersson, G. A.; Nakatsuji, H.; Hada, M.; Ehara, M.; Toyota, K.; Fukuda, R.; Hasegawa, J.; Ishida, M.; Nakajima, T.; Honda, Y.; Kitao, O.; Nakai, H.; Klene, M.; Li, X.; Knox, J. E.; Hratchian, H. P.; Cross, J. B.; Bakken, V.; Adamo, C.; Jaramillo, J.; Gomperts, R.; Stratmann, R. E.; Yazyev, O.; Austin, A. J.; Cammi, R.; Pomelli, C.; Ochterski, J. W.; Ayala, P. Y.; Morokuma, K.; Voth, G. A.; Salvador, P.; Dannenberg, J. J.; Zakrzewski, V. G.; Dapprich, S.; Daniels, A. D.; Strain, M. C.; Farkas, O.; Malick, D. K.; Rabuck, A. D.; Raghavachari, K.; Foresman, J. B.; Ortiz, J. V.; Cui, Q.; Baboul, A. G.; Clifford, S.; Cioslowski, J.; Stefanov, B. B.; Liu, G.; Liashenko, A.; Piskorz, P.; Komaromi, I.; Martin, R. L.; Fox, D. J.; Keith, T.; Al-Laham, M. A.; Peng, C. Y.; Nanayakkara, A.; Challacombe, M.; Gill, P. M. W.; Johnson, B.; Chen, W.; Wong, M. W.; Gonzalez, C.; Pople, J. A. *Gaussian03*, revision C.02; Gaussian Inc.: Wallingford, CT, 2004.

(17) Berces, A.; M. Z. Z.; Yang, D. S. *Computational Molecular Spectroscopy*; Wiley: New York, 2000; p 110.

(18) Yang, D.-S.; Zgierski, M. Z.; Rayner, D. M.; Hackett, P. A.; Martinez, A.; Salahub, D. R.; Roy, P.-N.; Carrington, T., Jr. *J. Chem. Phys.* **1995**, *103*, 5335.

(19) Duschinsky, F. *Acta Physicochim. URSS* **1937**, *7*, 551.

(20) Applegate, B. E.; Miller, T. A.; Barckholtz, T. A. *J. Chem. Phys.* **2001**, *114*, 4855.

(21) Applegate, B. E.; Bezant, A. J.; Miller, T. A. *J. Chem. Phys.* **2001**, *114*, 4869.

(22) Robles, E. S. J.; Ellis, A. M.; Miller, T. A. *J. Am. Chem. Soc* **1992**, *114*, 7171.

(23) Robles, E. S. J.; Ellis, A. M.; Miller, T. A. *J. Phys. Chem.* **1992**, *96*, 3247.

(24) Robles, E. S. J.; Ellis, A. M.; Miller, T. A. *J. Phys. Chem.* **1992**, *96*, 8791.

(25) Ellis, A. M.; Robles, E. S. J.; Miller, T. A. *J. Chem. Phys.* **1991**, *94*, 1752.

(26) O'Brien, L. C.; Bernath, P. F. *J. Am. Chem. Soc* **1986**, *108*, 5017.

(27) Coe, D. A.; Nibler, J. W.; Cook, T. H.; Drew, D.; Morgan, G. L. *J. Chem. Phys.* **1975**, *63*, 4842.

(28) Garkusha, O. G.; Lokshin, B. V.; Materikova, R. B.; Golubinskaya, L. M.; Bregadze, V. I.; Kurbakova, A. P. *J. Organomet. Chem.* **1988**, *342*, 281.

(29) Sado, A.; West, R.; Fritz, H. P.; Schafer, L. *Spectrochim. Acta* **1966**, *22*, 509.

(30) Rodenheimer, J. S.; Low, W. *Spectrochim. Acta* **1973**, *29*, 1733.

(31) Fritz, H. P. In *Advances in Organometallic Chemistry*; Stone, F. G. A., West, R., Eds.; Academic Press: London, 1964; Vol. 1, p 239.

(32) Bauschlicher, C. W.; Barnes, L. A.; Taylor, P. R. *J. Phys. Chem.* **1989**, *93*, 2932.

(33) Sunil, K. K.; Jordan, K. D. *J. Phys. Chem.* **1988**, *92*, 2774.

(34) Fu, Z.; Lemire, G. W.; Bishea, G. A.; Morse, M. D. *J. Chem. Phys.* **1990**, *93*, 8420.

(35) Langhoff, S. R.; Bauschlicher, J.; C. W. *J. Chem. Phys.* **1990**, *92*, 1879.

(36) Bauschlicher, J., C. W.; Partridge, H.; Langhoff, S. R.; Taylor, P. R.; Walch, S. P. *J. Chem. Phys.* **1987**, *86*, 7007.

(37) Lide, D. R.; Frederikse, H. P. R. *CRC Handbook of Chemistry and Physics*, 78th ed.; CRC: New York, 1997.

(38) Wörner, H. J.; Merkt, F. *Angew. Chem., Int. Ed.* **2006**, *45*, 293.

(39) Wang, X.; Yang, D.-S. *J. Phys. Chem. A* **2006**, *110*, 7568.

(40) Wang, X.; Lee, J. S.; Yang, D.-S. *J. Chem. Phys.* **2006**, *125*, 014309.

(41) Wang, X.; Lee, J. S.; Yang, D.-S. *J. Phys. Chem. A* **2006**, *110*, 12777.

(42) Miyawaki, J.; Sugawara, K.; Li, S.; Yang, D.-S. *J. Phys. Chem. A* **2005**, *109*, 6697.

(43) Wang, X.; Sohnlein B, R.; Li, S.; Fuller J, F.; Yang, D.-S. *Can. J. Chem.* **2007**, *85*, 714.

(44) Upton, T. H.; Cox, D. M.; Kaldor, A. In *Physics and Chemistry of Small Clusters*; Jena, P., Ed.; Plenum: New York, 1987; p 755.

(45) Hanley, L.; Ruatta, S. A.; Anderson, S. L. *J. Chem. Phys.* **1987**, *87*, 260.

(46) Jarrold, M. F.; Bower, J. E.; Kraus, J. S. *J. Chem. Phys.* **1986**, *86*, 3876.

(47) Yu, L.; Cullin, D. W.; Williamson, J. M.; Miller, T. A. *J. Chem. Phys.* **1993**, *98*, 2682.